A c-fms tyrosine kinase inhibitor, Ki20227, suppresses osteoclast differentiation and osteolytic bone destruction in a bone metastasis model

Hiroaki Ohno,[1] Kazuo Kubo,[1] Hideko Murooka,[1] Yoshiko Kobayashi,[1] Tsuyoshi Nishitoba,[1] Masabumi Shibuya,[2] Toshiyuki Yoneda,[3] and Toshiyuki Isoe[1]

[1]Pharmaceutical Research Laboratories, Pharmaceutical Division, Kirin Brewery Co., Ltd., Gunma, Japan; [2]Division of Genetics, Institute of Medical Science, University of Tokyo, Tokyo, Japan; and [3]Department of Biochemistry, Osaka University Graduate School of Dentistry, Osaka, Japan

Abstract

In bone metastatic lesions, osteoclasts play a key role in the development of osteolysis. Previous studies have shown that macrophage colony-stimulating factor (M-CSF) is important for the differentiation of osteoclasts. In this study, we investigated whether an inhibitor of M-CSF receptor (c-Fms) suppresses osteoclast-dependent osteolysis in bone metastatic lesions. We developed small molecule inhibitors against ligand-dependent phosphorylation of c-Fms and examined the effects of these compounds on osteolytic bone destruction in a bone metastasis model. We discovered a novel quinoline-urea derivative, Ki20227 (*N*-{4-[(6,7-dimethoxy-4-quinolyl)oxy]-2-methoxyphenyl}-*N*′-[1-(1,3-thiazole-2-yl)ethyl]urea), which is a c-Fms tyrosine kinase inhibitor. The IC_{50}s of Ki20227 to inhibit c-Fms, vascular endothelial growth factor receptor-2 (KDR), stem cell factor receptor (c-Kit), and platelet-derived growth factor receptor β were found to be 2, 12, 451, and 217 nmol/L, respectively. Ki20227 did not inhibit other kinases tested, such as fms-like tyrosine kinase-3, epidermal growth factor receptor, or c-Src (*c-src* proto-oncogene product). Ki20227 was also found to inhibit the M-CSF-dependent growth of M-NFS-60 cells but not the M-CSF-independent growth of A375 human melanoma cells *in vitro*. Furthermore, in an osteoclast-like cell formation assay using mouse bone marrow cells, Ki20227 inhibited the development of tartrate-resistant acid phosphatase–positive osteoclast-like cells in a dose-dependent manner. In *in vivo* studies, oral administration of Ki20227 suppressed osteoclast-like cell accumulation and bone resorption induced by metastatic tumor cells in nude rats following intracardiac injection of A375 cells. Moreover, Ki20227 decreased the number of tartrate-resistant acid phosphatase–positive osteoclast-like cells on bone surfaces in ovariectomized (ovx) rats. These findings suggest that Ki20227 inhibits osteolytic bone destruction through the suppression of M-CSF-induced osteoclast accumulation *in vivo*. Therefore, Ki20227 may be a useful therapeutic agent for osteolytic disease associated with bone metastasis and other bone diseases. [Mol Cancer Ther 2006; 5(11):2634–43]

Introduction

Bone metastasis of tumor cells is a clinical complication frequently associated with breast, lung, and prostate cancers (1). In the process of bone metastasis, metastatic tumor cells in bone enhance osteolysis by inducing and activating osteoclastic bone resorption through the signaling pathway mediated by parathyroid hormone-related peptide (PTHrP) or through the receptor activator of nuclear factor κB ligand (RANKL; refs. 2, 3). It has also been reported that transforming growth factor-β (TGF-β), which is stored in bone matrix and released by osteoclastic bone resorption, brings about enhanced PTHrP production of tumor cells in bone (4). Increased production of PTHrP accelerates further bone resorption and provides more space for tumor cell proliferation. Suppression of osteoclastic bone resorption may, therefore, be effective against bone metastasis. In studies using rodent bone metastasis models, bisphosphonate, osteoprotegerin, anti-PTHrP-neutralizing antibody, tissue inhibitor of matrix metalloproteinase-2, and angiogenesis inhibitor have all been found to suppress osteolytic bone metastasis (2, 5–11). Bisphosphonates exert an inhibitory action on mature osteoclasts and suppress bone resorption enhanced by metastatic tumor cells by inducing apoptosis of osteoclasts (12, 13). Osteoprotegerin is a member of the tumor necrosis factor receptor family, which antagonizes the ability of RANKL by suppressing binding to its receptor RANK (14–19). The administration of osteoprotegerin or bisphosphonates suppresses osteolytic bone metastasis.

Osteoclasts are derived from monocytic progenitor cells and experimentally differentiate from spleen and bone marrow cells in the simultaneous presence of macrophage colony-stimulating factor (M-CSF) and RANKL *in vitro* (16). M-CSF-deficient osteopetrotic (*op/op*) mice suffer severe osteopetrosis because of the depletion of osteoclasts; however, this pathologic condition is improved by the

Received 8/10/06; revised 9/1/06; accepted 9/25/06.

The costs of publication of this article were defrayed in part by the payment of page charges. This article must therefore be hereby marked advertisement in accordance with 18 U.S.C. Section 1734 solely to indicate this fact.

Requests for reprints: Hiroaki Ohno, Pharmaceutical Research Laboratories, Kirin Brewery Co., Ltd., 3 Miyahara, Takasaki, Gunma, 370-1295, Japan. Phone: 81-27-346-9815; Fax: 81-27-346-1672. E-mail: h-ohno@kirin.co.jp

doi:10.1158/1535-7163.MCT-05-0313

administration of M-CSF (20–23). A recent report on M-CSF receptor (c-Fms)–null mice also found a severe deficiency of osteoclasts and abnormal skeletal development, as found in *op/op* mice (24). These data strongly suggest that M-CSF is essential for the development of osteoclasts *in vivo*, and that the suppression of the M-CSF/c-Fms signaling pathway is also effective against bone metastasis. In our present study, we examined the inhibitory effects of Ki20227, a c-Fms inhibitor, on the development of tartrate-resistant acid phosphatase (TRAP)–positive osteoclast-like cells and osteolytic bone destruction induced by the A375 human melanoma cell line.

Materials and Methods

Ki20227

Ki20227 (*N*-{4-[(6,7-dimethoxy-4-quinolyl)oxy]-2-methoxyphenyl}-*N*′-[1-(1,3-thiazole-2-yl)ethyl]urea; racemic) and its enantiomers were synthesized in the Kirin Pharmaceutical Research Laboratories (Gunma, Japan). The racemic form is called Ki20227, and its enantiomers are dubbed (*R*)-Ki20227 and (*S*)-Ki20227. For *in vitro* studies, compounds were dissolved in DMSO and diluted in growth medium immediately before use. As a rule, the concentration of DMSO was 0.5% in all *in vitro* assays. For *in vivo* studies, Ki20227 was suspended in vehicle (0.5% methyl cellulose in distilled water).

Cell Lines and Cultures

RAW264.7 (a mouse macrophage cell line) and THP-1 (a human monocytic cell line) were obtained from Dainippon Pharmaceutical Co., Ltd. (Osaka, Japan). M-NFS-60 mouse myelogenous leukemia cell line was obtained from the American Type Culture Collection (Manassas, VA), and human umbilical vein endothelial cells (HUVEC) were obtained from Cambrex (Walkersville, MD). RAW264.7 and A375 were maintained in DMEM (Invitrogen Corp., Carlsbad, CA) containing 10% FCS at 37°C in 5% CO_2 in a water-saturated atmosphere. THP-1 cells were maintained in RPMI 1640 (Invitrogen) containing 10% FCS. M-NFS-60 cells were maintained in RPMI 1640 containing 10% FCS in the presence of 50 ng/mL M-CSF (R&D Systems, Inc., Minneapolis, MN). HUVEC cells were cultured in EGM-2 (Cambrex).

Animals

All *in vivo* experiments were conducted under Kirin Animal Care and Use Committee guidelines. All animals were housed in a barrier facility with a 12-hour light/dark cycle and were provided with sterilized food and water *ad libitum*. We obtained ddY mice for the osteoclast-like cell formation assay from Japan SLC, Inc. (Hamamatsu, Japan). Athymic rats (F344/NJcl-rnu) for the bone metastasis model were obtained from CLEA Japan, Inc. (Tokyo, Japan). For the ovx model, Sprague-Dawley rats were used (Japan SLC).

Inhibitory Effects of Ki20227 against Protein Kinases

IC_{50}s of Ki20227, (*R*)-Ki20227, and (*S*)-Ki20227 for inhibition of protein kinases were determined using IC_{50} profiler Express (Upstate Ltd., Dundee, United Kingdom). Cell-free kinase inhibition assays against c-Fms, Bruton's tyrosine kinase, KDR, c-Kit, platelet-derived growth factor receptor β, fms-like tyrosine kinase-3, c-Src, Fyn, epidermal growth factor receptor, basic fibroblast growth factor receptor 2, hepatocyte growth factor/scatter factor receptor (c-Met), protein kinase A, and protein kinase Cα were done. All kinases are human derived.

Western Blotting

RAW264.7 cells were serum starved for 12 hours in DMEM containing 0.1% FCS. Serial dilutions of Ki20227 were then added to the cells, and they were incubated for 1 hour. RAW264.7 cells were stimulated with 50 ng/mL of recombinant mouse M-CSF for 4 minutes. c-Fms protein in the RAW264.7 cell lysate was prepared with ice-cold lysis buffer [50 mmol/L Tris/HCl (pH 7.4), 150 mmol/L NaCl, 1.0 mmol/L NaF, 0.1% sodium deoxycholate, 4 mmol/L EDTA, 1.0 mmol/L Na_3VO_4, 1 mmol/L phenylmethylsulfonyl fluoride, 1 μg/mL aprotinin, 1% NP40]. Lysates were immunoprecipitated with rabbit polyclonal antibody to c-Fms (C-20; Santa Cruz Biotechnology, Inc., Santa Cruz, CA), subjected to SDS-PAGE, and transferred to a polyvinylidene fluoride microporous membrane. The membrane was probed with phosphotyrosine antibody PY20 (Transduction Laboratories, Lexington, KY), and phosphorylation was detected with peroxidase-conjugated anti-immunoglobulin G (Amersham Biosciences, Inc., Piscataway, NJ). After the PY20 was removed, the same membrane was probed with anti-c-Fms antibody (C-20) following the same protocol.

In vitro Growth Inhibition Assay

M-NFS-60, HUVEC, and A375 cells were seeded on a 96-well culture plate and cultured for 24 hours. Then, culture mediums were changed and incubated for a further 72 hours in the presence or absence of test compounds (0.1–3,000 nmol/L). The detail were as follows: M-NFS-60 cells were seeded at a density of 5.0×10^3 per well in DMEM supplemented with 10% FCS and 50 ng/mL recombinant mouse M-CSF, and the culture medium was changed to DMEM supplemented with 3% FCS and 50 ng/mL recombinant mouse M-CSF. HUVEC cells were planted at 2.0×10^3 per well in EGM-2, and the culture medium was changed to EBM-2 (Cambrex) supplemented with 3% FCS and 20 ng/mL recombinant human vascular endothelial growth factor (VEGF; Peprotech EC, Ltd., London, United Kingdom). A375 cells were planted at a density of 2.0×10^3 per well in DMEM supplemented with only 10% FCS, and the culture medium was changed to DMEM supplemented with 3% FCS; similar growth inhibition assay was done as described above. After 72 hours of incubation, 3-(4,5-dimethylthiazol-2-yl)-5-(3-carboxymethoxyphenyl)-2-(4-sulfophenyl)-2*H*-tetrazolium reagent (Promega Corp., Madison, WI) was added to each well and incubated at 37°C for 2 hours, and growth inhibition activity was then calculated by measurement of absorbance at 490 nm.

Osteoclast-Like Cell Formation Assay

The osteoclast-like cell formation assay was done following the method previously reported by Kobayashi

et al. (25), with some modification. In a 48-well culture plate, the mouse femoral bone marrow cells (1.5×10^5) from 4-week-old male ddY mice were cultured in αMEM supplemented with 10% FCS and 100 ng/mL recombinant mouse M-CSF for 72 hours in the presence or absence of test compounds. The medium was changed to αMEM supplemented with 10% FCS, 20 ng/mL recombinant mouse M-CSF, and 100 ng/mL recombinant mouse soluble RANKL (sRANKL; Peprotech), and the cells were cultured for a further 72 hours with or without test compounds. When the culture was terminated, the cells were fixed, and TRAP staining was done using a staining kit (acid phosphatase, leukocyte; Sigma Chemical Co., St. Louis, MO). The TRAP-positive cells containing two or more nuclei under microscopy were counted as osteoclast-like cells. The inhibitory effect of Ki20227 on the development of osteoclast-like cells was evaluated with the number of TRAP-positive cells.

Intracardiac Injections of A375 Cells in Nude Rats

A375 cells (5.0×10^5) were suspended in 0.1 mL of PBS and inoculated into the left cardiac ventricle of 4-week-old, male F344/NJcl-rnu rats ($n = 8$ animals for each group) with a 26-gauge needle under anesthesia (75 mg/kg keamine, 0.5 mg/kg medetomidine). Sham-operated rats ($n = 3$) were injected with an equivalent volume of PBS only. Beginning on the day after inoculation, Ki20227 (10, 20, and 50 mg/kg/d) or 0.5% CMC-Na were given orally once per day for 20 days.

X-ray Analysis of Bone Metastasis

Twenty-one days after the injection of A375 cells, the formation of bone metastases was examined on soft X-ray images. The rats were deeply anesthetized, laid down in a prone position against the imaging plate (Fuji Photo Film Co., Ltd., Tokyo, Japan), and exposed to a soft X-ray at 40 kV for 10 seconds with μFX-1000 (Fuji). The radiographs were scanned with a BAS-2500 IP Reader (Fuji), and the total osteolytic lesion areas and total lesion number in the femorae and tibiae of each animal were measured using ImageGauge digital image analysis software (Fuji).

Ovariectomized Rat Model

Ki20227 (20 mg/kg/d) was given orally once per day for 28 days to 6-week-old female Sprague-Dawley rats ($n = 6$ animals for each group). Seven days after the first administration of Ki20227 (day 7), the rats were either ovx or sham operated. The vehicle-treated ovx-operated and sham-operated groups received 0.5% CMC-Na. At 21 days after surgery (day 28), the rats were sacrificed, and the tibiae were removed. Whether or not ovx was successful was confirmed by measurement of the weight of the uterus upon dissection on day 28 (data not shown).

Histologic and Histochemical Examination

The hind limbs of bone metastasis and ovariectomized rats were fixed in 10% neutral phosphate-buffered formalin. The specimens were decalcified in a 10% EDTA solution for 2 weeks and embedded in paraffin. The paraffin-embedded specimens were then sectioned at intervals of 5 μm and stained following conventional methods with H&E. Histochemical examination for TRAP was also done following standard methods using Naphthol AS-MX phosphoric acid.

Histomorphometric Analysis

In the bone metastasis model, histomorphometric analysis of tumor burden in both tibiae was done using longitudinal sections stained with H&E (×40 magnification). Tissue area occupied by metastatic tumor cells was measured using a digital camera system combined with microscopy (DP70; Olympus Corp., Tokyo, Japan) and image analyzing software (WinROOF, version 5.5; Mitani Corp., Fukui, Japan). The number of TRAP-positive multinucleated cells at the tumor bone interface in the metastatic bone in the proximal tibial metaphyses and at the bone surface in primary spongiosa in both tibiae in the ovariectomized rat model were counted in five field for each section (×400 magnification).

Bone Resorption Marker

Bone resorption marker (TRAP-5b) was measured at the end of the experiment in the bone metastasis rat serum using an ELISA kit (RatTRAP Assay; Suomen Bioanalytiikka Oy SBA Science, Turku, Finland) according to the manufacturer's instructions. Rat serum samples were tested in duplicate.

Analysis of c-fms Expression

To prepare the metastasized tumor RNA, both left and right rat tibiae were isolated, and the metaphysial portions, including tumor and bone marrow, were excised and frozen. The frozen bone tissue with tumor and bone marrow was crushed and homogenized to purify total RNA using the RNeasy Mini kit (Qiagen, Valencia, CA). The corresponding portion of bones in the normal rats were isolated, and total RNA was similarly prepared. The cultured A375 and THP-1 cells were lysed, and total RNA was extracted. All purified total RNAs were treated with DNase (Qiagen) to remove genomic DNA contamination, followed by first-strand cDNA synthesis using a random hexamer and the SuperScript III First Strand Synthesis System (Invitrogen). The first-strand cDNAs obtained were amplified by real-time quantitative PCR on an ABI 7900 (Applied Biosystems, Inc., Foster City, CA) using the QuantiTect SYBR Green PCR kit (Qiagen). Primer pairs used are commercially available Perfect Real-time Primers (TAKARA Bio, Inc., Shiga, Japan), with the following ID nos.: HA040814 for human c-fms; HA036137 for human MHC, class I, A (HLA-A); and HA031582 for human β-actin.

Statistical Analysis

All data were analyzed by Dunnett's test using StatLight statistical software (Yukms Co., Ltd., Tokyo, Japan). All data are presented as the mean ± SE.

Results

Inhibitory Activity of Ki20227 against Protein Kinases

Ki20227 was synthesized as an inhibitor of c-Fms tyrosine kinase (Fig. 1). The IC_{50}s of Ki20227 to inhibit c-Fms, KDR, c-Kit, and platelet-derived growth factor receptor β are 2, 12, 451, and 217 nmol/L, respectively (Table 1). In

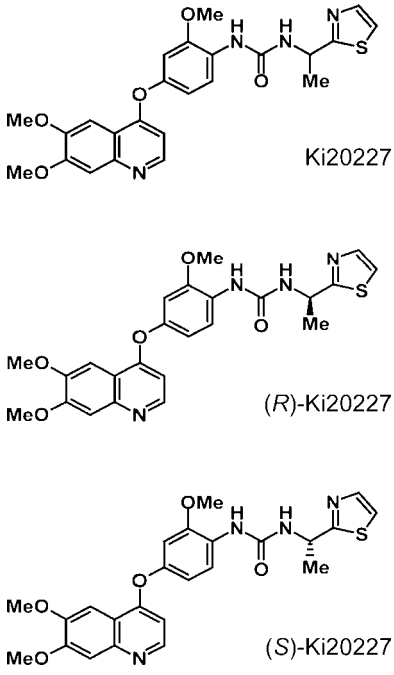

Figure 1. Chemical structure of Ki20227, (*R*)-Ki20227, and (*S*)-Ki20227.

contrast, the IC_{50}s for fms-like tyrosine kinase-3, c-Src, Fyn, epidermal growth factor receptor, fibroblast growth factor receptor 2, Met, Bruton's tyrosine kinase, protein kinase A, and protein kinase Cα were all >1,000 nmol/L (Table 1). The IC_{50} profiles of both (*R*)-Ki20227 and (*S*)-Ki20227 for protein kinases also show the same tendencies as Ki20227 (Table 1).

Effect of Ki20227 in Cell-Based Assays

Western blotting analysis and cell growth determinations were used to evaluate the inhibitory activity of Ki20227 in response to M-CSF in cell-based assays. Western blotting showed that Ki20227 could inhibit M-CSF-dependent c-Fms phosphorylation in a dose-dependent manner in RAW264.7 cells cultured in medium supplemented with 0.1% FCS (Fig. 2A). The inhibitory activity of Ki20227 against M-CSF-dependent and VEGF-dependent cell growth was examined using M-NFS-60 and HUVEC cells (Fig. 2B). The addition of M-CSF and VEGF to medium supplemented with 3% FCS is essential for M-NFS-60 cell and HUVEC cell growth, respectively. Growth of M-NFS-60 cells in medium supplemented with 3% FCS and 50 ng/mL M-CSF was almost completely suppressed by treatment with 100 nmol/L of Ki20227. However, growth suppression in HUVEC cells grown in medium supplemented with 3% FCS and 20 ng/mL VEGF required treatment with 1,000 nmol/L of Ki20227. The IC_{50}s of Ki20227 for M-NFS-60 cells and HUVEC cells were ~14 and 500 nmol/L. However, these inhibitory effects are significantly different from those seen in an *in vitro* kinase inhibition assay (c-Fms, 2 nmol/L; KDR, 12 nmol/L). This may be explained by the fact that Ki20227 is a highly protein-bound compound, as determined by Biacore analysis. Human and rat albumin-binding ratios of Ki20227 were no less than 95% (data not shown). This nonspecific serum protein binding of Ki20227 may account for the differences in activity between cell-free and cell-based assays. Another explanation for this phenomenon may be a direct growth stimulation by FCS in these cultures. In this context, it is possible that M-CSF and VEGF are merely modulators of cell proliferation in these assays. Hence, the proliferation of these cells maybe an indirect index of ligand action, and a higher concentration of Ki20227 may thus be required to suppress M-NFS-60 and HUVEC cell growth.

The inhibitory activities of (*R*)-Ki20227 and (*S*)-Ki20227 against M-NFS-60, HUVEC, and A375 cell growth were similar to Ki20227 (Fig. 2B). These data show the inhibitory effects of these compounds against kinases in both cell-based and cell-free assays.

Suppression of the Development of TRAP-Positive Osteoclast-Like Cells

To evaluate whether the inhibition of c-Fms kinase leads to the suppression of the development of TRAP-positive osteoclast-like cells, mouse bone marrow culture using M-CSF and sRANKL was done. Mouse bone marrow cells were cultured with various doses of the compounds [Ki20227, (*R*)-Ki20227, and (*S*)-Ki20227] for 6 days in the presence of M-CSF and sRANKL. These chemicals suppressed the development of TRAP-positive osteoclast-like cell formation in a dose-dependent manner, and this development was almost completely suppressed by treatment with 100 nmol/L of each compound (Fig. 3A and B). The IC_{50}, calculated by the number of TRAP-positive osteoclast-like cells in cultures on day 6, was found to be ~40 nmol/L.

Table 1. Inhibitory effects of Ki20227 on kinases

Kinase	IC_{50} (nmol/L)		
	Ki20227	(*R*)-Ki20227	(*S*)-Ki20227
c-Fms	2	3	1
KDR	12	7	12
c-Kit	451	447	244
PDGFRβ	217	363	423
Flt3	>1,000	>1,000	>1,000
c-Src	>1,000	>1,000	>1,000
Fyn	>1,000	>1,000	>1,000
EGFR	>1,000	>1,000	>1,000
FGFR2	>1,000	>1,000	>1,000
Met	>1,000	>1,000	>1,000
BTK	>1,000	>1,000	>1,000
PKA	>1,000	>1,000	>1,000
PKCα	>1,000	>1,000	>1,000

NOTE: IC_{50}s were determined by IC_{50} Profiler Express.

Abbreviations: PDGFRβ, platelet-derived growth factor receptor β; Flt3, fms-like tyrosine kinase-3; EGFR, epidermal growth factor receptor; FGFR2, fibroblast growth factor receptor 2; BTK, Bruton's tyrosine kinase; PKA, protein kinase A; PKCα, protein kinase Cα.

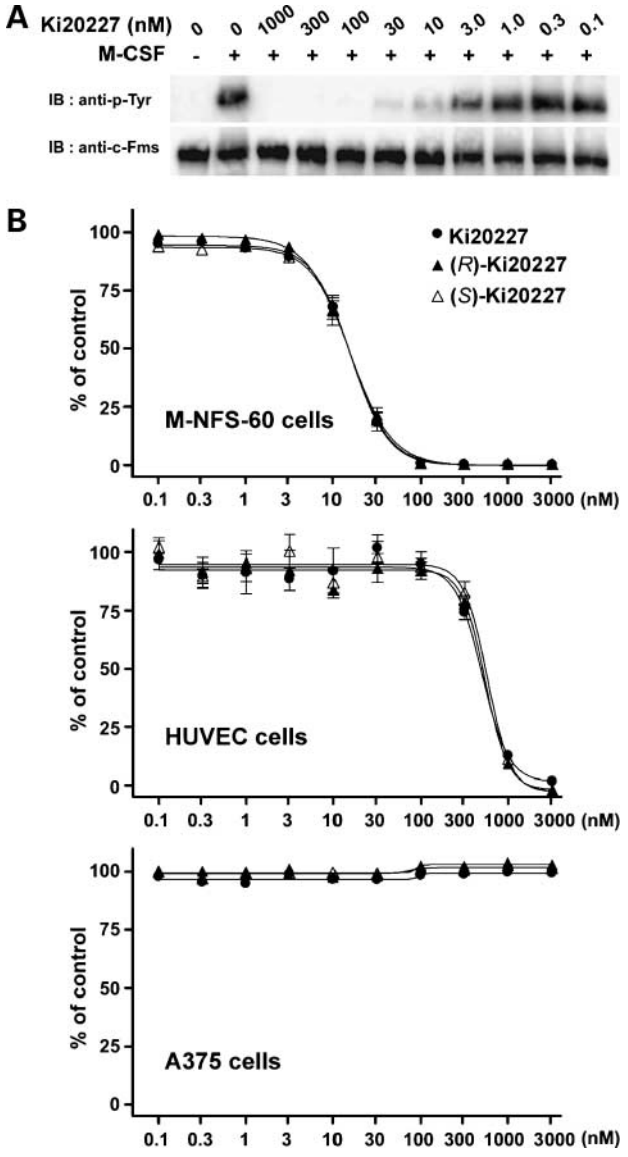

Figure 2. **A,** effects of Ki20227 on c-Fms phosphorylation. C-Fms protein in the RAW264.7 cell lysate was immunoprecipitated with anti-c-Fms antibody and subjected to SDS-PAGE. The phosphorylation levels of c-Fms were detected by immunoblotting with anti-phosphotyrosine monoclonal antibody (*top*) and anti-c-Fms antibody (*bottom*). Ki20227 suppressed M-CSF-dependent c-Fms phosphorylation in a dose-dependent manner. **B,** effects of Ki20227 on M-CSF-dependent growth of M-NFS-60 cells, vascular endothelial growth factor–dependent growth of HUVEC cells, and human A375 melanoma cells *in vitro*. Cells were incubated at 37°C for 72 h in the presence or absence of the test compound. M-NFS-60 cell growth and HUVEC cell growth were almost suppressed by treatment with 100 and 1,000 nmol/L of Ki20227, respectively. However, M-CSF-independent growth of A375 cells was not suppressed at 3,000 nmol/L. The IC_{50} of Ki20227 for M-NFS-60 growth was ~14 nmol/L. *Points,* mean (n = 4 for each experiment); *bars,* SE.

Inhibitory Effects of Ki20227 on Osteolytic Bone Metastasis in Nude Rats

Based on our *in vitro* data, we concluded that the biological activities of Ki20227, (*R*)-Ki20227, and (*S*)-Ki20227 were nearly identical; therefore, we chose to use only Ki20227 for further *in vivo* studies. Twenty-one days after the intracardiac injection of A375 cells into nude rats, osteolytic lesions were analyzed by X-ray. Radiographs showed that the tumor cells had aggressively metastasized to bones, such as femurs, tibiae, jawbones, and pelvises, in all A375-injected animals (Fig. 4A, *a*; data not shown). However, oral administration of 50 mg/kg/d of Ki20227

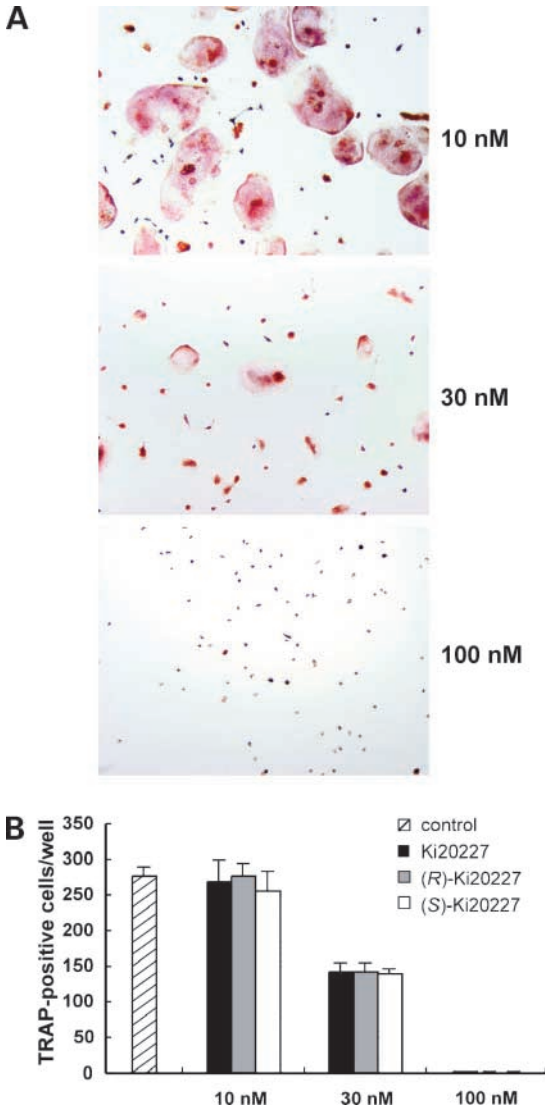

Figure 3. Effect of Ki20227 treatment on the development of TRAP-positive osteoclast-like cells. Bone marrow cells were cultured for 6 d with or without the addition of the indicated compounds. When the culture was terminated, the cells were fixed, and TRAP staining was done. **A,** micrographs of cultures incubated with 10, 30, and 100 nmol/L Ki20227. The development of TRAP-positive osteoclast-like cells (*red*) was suppressed by the addition of Ki20227 in a dose-dependent manner. **B,** TRAP-positive cells number in these cultures on day 6. Under microscopy, the TRAP-positive cells containing two or more nuclei were counted as osteoclast-like cells. The IC_{50}s of Ki20227, (*R*)-Ki20227, and (*S*)-Ki20227 for the development of TRAP-positive osteoclast-like cells were ~40 nmol/L. *Columns,* mean (n = 4 for each experiment); *bars,* SE.

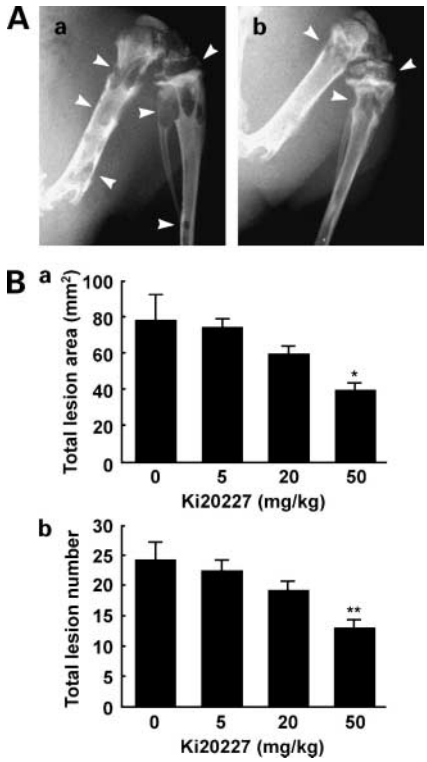

Figure 4. **A,** representative radiographs of A375 tumor-induced osteolytic lesions of vehicle-treated (**a**) or Ki20227-treated (50 mg/kg/d; **b**) nude rats on day 21. Osteolytic lesions (*arrowheads*) were observed in both groups, but osteolysis induced by metastatic A375 cells was significantly suppressed in Ki20227-treated rats. **B,** the total area of osteolytic lesions (mm^2/head; **a**) and total lesion number (**b**) in right and left femora and tibiae of each animal were measured on the radiographs at day 21. Ki20227 significantly reduced both the total area and number of osteolytic lesions at a dose of 50 mg/kg/d. *Columns,* mean ($n = 8$ animals for each group); *bars,* SE. *, $P < 0.05$; **, $P < 0.01$, compared with vehicle-treated group.

for 20 days markedly decreased the osteolytic lesion areas (Fig. 4A, *b*). Measurement of the total osteolytic lesion areas in femurs and tibiae revealed that treatment with 50 mg/kg/d of Ki20227 significantly decreased the lesion areas, whereas doses of 5 or 20 mg/kg/d did not (Fig. 4B, *a*).

The total number of osteolytic lesions in femurs and tibiae were also significantly suppressed by treatment with 50 mg/kg/d Ki20227 but not with lower doses (Fig. 4B, *b*). Histologic examination of the tibiae in these animals revealed that the bone marrow cavity was almost completely replaced by metastatic A375 cells (*T*) in vehicle-treated rats, and many TRAP-positive cells were observed at the interface between metastatic tumor and bone surface (Fig. 5A, *a*). In contrast, it was found that the number of TRAP-positive osteoclastic cells were reduced, and the structure of cancellous bone in the proximal tibiae and epiphysis was maintained in Ki20227-treated rats (Fig. 5A, *b*). In the 50 mg/kg/d Ki20227-treated group, an A375 tumor burden was observed; however, the colonization of metastatic A375 cells in the bone marrow cavity and the number of TRAP-positive cells were significantly decreased (Fig. 5B and C).

Serum TRAP-5b levels in the vehicle-treated A375 tumor-bearing rats markedly increased compared with levels in the sham non–tumor-bearing group. However, this increased TRAP-5b level, derived from bone-resorbing osteoclasts, was significantly decreased in the 50 mg/kg/d Ki20227-treated tumor-bearing group (Fig. 5D). These suppressions (colonization, osteoclast number, and TRAP-5b level) were not observed in either the 5 or 20 mg/kg/d treated rats (data not shown). Taken together, these data suggest that osteoclast activity is diminished by treatment with 50 mg/kg/d of Ki20227.

PCR Analysis of the Expression of c-Fms in Metastatic Tumor Cells

Ki20227 suppressed M-CSF-dependent M-NFS-60 cell growth; however, A375 cell proliferation was not inhibited in an *in vitro* cell growth assay. It was predicted that the behavior of metastatic A375 cells in the bone microenvironment would be different from their growth in *in vitro* cultures. If A375 cells in bone express c-Fms at higher levels than in culture, Ki20227 might have a greater effect on the growth of A375 cells in bone and might suppress osteolysis through a direct antiproliferative effect in these cells.

To determine whether the expression levels of c-Fms were maintained in metastatic A375 cells, we measured human c-Fms expression in metastatic A375 cells by real-time quantitative PCR analysis. We could detect high expression of human c-Fms only in THP-1 cells cultured *in vitro* (Fig. 6A). Both cultured and metastatic A375 cells in rat bone had barely detectable levels of c-Fms, and there were no PCR product detected in normal rat bone. Human HLA-A expression was detectable in all RNA samples except normal rat bone (Fig. 6B), indicating that we could observe c-Fms expression of metastatic A375 cells in rat bone. The higher expression of HLA-A found in metastatic A375 cells in bone may be due to phenotypic changes in these cells in bone microenvironment. c-Fms expression was not found to be up-regulated in metastatic A375 in bone compared with A375 cells in culture. Therefore, we conclude that the inhibitory effects of Ki20227 upon osteolysis, induced by metastatic tumor cells, is not through a direct antiproliferative effect on metastatic A375 cells.

Osteoclastic Cells in Bones from Ovariectomized Rats

It has been indicated that Ki20227 inhibits osteolysis via the suppression of the development of osteoclasts induced by tumor cells based on a bone metastasis rat model. To confirm the inhibitory effect of Ki20227 against osteoclast development in rats, we investigated the effects of this compound in a rat ovx model. Ki20227 and vehicle were given orally for 28 days, beginning at 7 days before surgery. The numbers of TRAP-positive cells on the bone surface in the vehicle-treated (Fig. 7A, *a*) and the Ki20227-treated group (Fig. 7A, *b*) were then determined. Once-daily oral administration of Ki20227 at 20 mg/kg significantly decreased the number of TRAP-positive osteoclastic cells on the bone surface (OcN/mm bone surface) in the primary

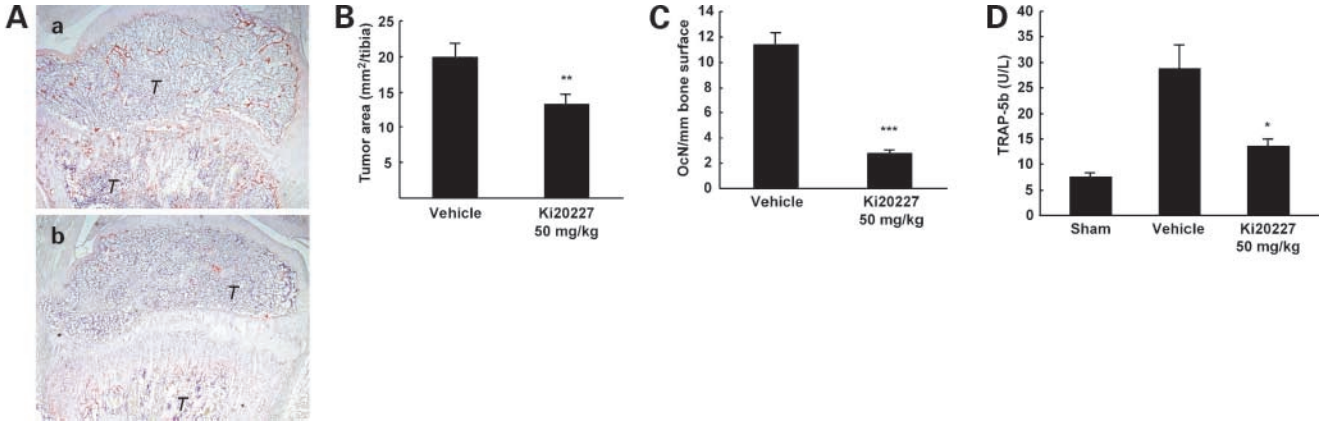

Figure 5. **A,** histologic appearance of the proximal ends of tibiae stained for TRAP in vehicle-treated (**a**) and Ki20227-treated (50 mg/kg/d; **b**) A375 tumor-bearing rats. In both groups, metastatic tumor cells (*T*) were observed. However, Ki20227 reduced the number of TRAP-positive osteoclastic cells (*red*) and maintained the bone structures in the epiphysis and proximal tibia. Tumor area (mm^2/tibia; **B**) and the number of TRAP-positive cells at the tumor bone interface (OcN/mm bone surface; **C**) were measured via microscopy. Ki20227 significantly reduced the tumor area and the number of TRAP-positive cells on the bone surface at a dose of 50 mg/kg/d. Moreover, the bone resorption marker (serum TRAP-5b levels of 50 mg/kg/d) of the Ki20227-treated group was also significantly reduced compared with the vehicle-treated group (**D**). *Columns,* mean ($n = 3$ animals for sham group, $n = 8$ animals for vehicle-treated and Ki20227-treated group); *bars,* SE. *, $P < 0.05$; **, $P < 0.01$; ***, $P < 0.001$, compared with vehicle-treated group.

spongiosa compared with that in the vehicle-treated group (Fig. 7B). These data indicate that Ki20227 suppresses TRAP-positive osteoclast-like cell development in a non–tumor-bearing rodent model.

Discussion

Many small molecule inhibitors of tyrosine kinases, such as epidermal growth factor, VEGF, and platelet-derived growth factor receptors, have been reported, and some inhibitors have been advanced in clinical trials or placed on the market (26). In the present study, we describe a c-Fms inhibitor and show that this compound inhibits osteoclast development both *in vitro* and *in vivo*, as well as suppressing metastatic tumor-induced osteolysis.

M-CSF regulates the monocytic lineage, including osteoclast development *in vivo* (27). Additionally, it increases isolated osteoclast survival *in vitro* and induces the development of bone marrow cells to osteoclasts in the presence of RANKL *in vitro* (16, 28). In *in vivo* studies, *op/op* mice develop osteopetrosis due to a severe deficiency of osteoclasts caused by the absence of functional M-CSF (20, 21). The administration of M-CSF has been found to significantly improve this pathologic condition due to the resultant increase in osteoclasts (22, 23). A recent report showed that c-Fms-null mice have the same phenotype (24). These data suggest that M-CSF plays an essential role in osteoclast development both *in vivo* and *in vitro*. In our present study, we show that Ki20227, (*R*)-Ki20227, and (*S*)-Ki20227 suppress TRAP-positive osteoclast-like cell formation in a dose-dependent manner in bone marrow culture using M-CSF and sRANKL, with IC_{50}s ~40 nmol/L. This concentration is similar to the dose required to achieve the inhibitory effects against M-CSF-dependent growth of M-NFS-60. Thus, the inhibitory effect against osteoclast formation in this bone marrow culture system using M-CSF and sRANKL is most likely not due to cytotoxicity.

Breast, prostate, and lung cancers are frequently associated with bone metastasis. In the process of bone metastasis, metastatic tumor cells enhance osteolysis through various factors, such as PTHrP and TGF-β (2, 4). In the case of the human breast cancer cell line (MDA-MB-231), it is reported that PTHrP, produced by metastatic MDA-MB-231 cells in bone, is enhanced by TGF-β. TGF-β is released by osteoclasts from the bone matrix, and the increased secretion of PTHrP then induces greater osteoclast activation and bone destruction (4). These data indicate that PTHrP and TGF-β contribute to a vicious cycle of bone destruction and tumor growth in bone. Previous studies have shown that M-CSF antiserum suppresses osteoclast development and osteoclastic bone resorption induced by PTHrP, and that M-CSF expression by MDA-MB-231 cells is significantly higher in bone metastatic sites than in soft tissues (29, 30). These data, thus, indicate that the M-CSF/c-Fms pathway plays an important role in the formation of this detrimental cycle involving PTHrP.

The A375 human melanoma cell line is as well characterized as MDA-MB-231 cells in forming tumors in rodent bone metastasis models (31). A375 induces bone resorption by secreting osteotropic cytokines, such as interleukin-6, prostaglandin E_2, TGF-α (32), and PTHrP (33), indicating that A375 cells have various abilities for enhancing osteoclast development and bone resorption, although the involvement of M-CSF in the bone metastasis of A375 cells remains uncertain. However, the data showing that A375 cells produce PTHrP, in a similar manner to MDA-MB-231 cells, indicate that PTHrP works in conjunction with M-CSF in osteoclast accumulation induced by metastatic A375 cells. Moreover, it is expected

that M-CSF antagonists would suppress these osteoclast accumulations.

In the present study, we investigated whether the c-Fms inhibitor Ki20227 suppresses osteoclast accumulation and osteolytic bone destruction induced by A375 cells. Our *in vitro* data, including a cell-free kinase assay and cell-based assay, indicate that the biological activities of Ki20227, (*R*)-Ki20227, and (*S*)-Ki20227 are nearly identical; thus, our subsequent *in vivo* studies focused on racemic Ki20227. In untreated animals, aggressive bone metastasis of A375 cells occurred in the hind limbs within 3 weeks of intracardiac injection. X-ray analysis revealed that once-daily oral administration of 50 mg/kg of Ki20227 significantly reduced the osteolytic lesion area and lesion numbers in the femurs and tibiae. Histologic analysis showed the presence of many osteoclasts and severe bone resorption near the metastatic tumor cells and tumor colonization in the bone cavity in the vehicle-treated group. We found that Ki20227 suppresses the osteoclast accumulation induced by metastatic tumor cells in bone and also suppresses tumor colonization to a lesser extent. We thus hypothesize that tumor growth in the bone cavity is partially osteoclast independent. On the other hand, the serum concentration of the bone resorption marker TRAP-5b was also decreased in the Ki20227-treated group. From these data, the inhibitory effects of Ki20227 on osteolysis and tumor colonization seemed to be caused by the suppression of the development of TRAP-positive osteoclast-like cells. However, there remained a possibility that Ki20227 directly inhibited metastatic A375 growth in the bone microenvironment.

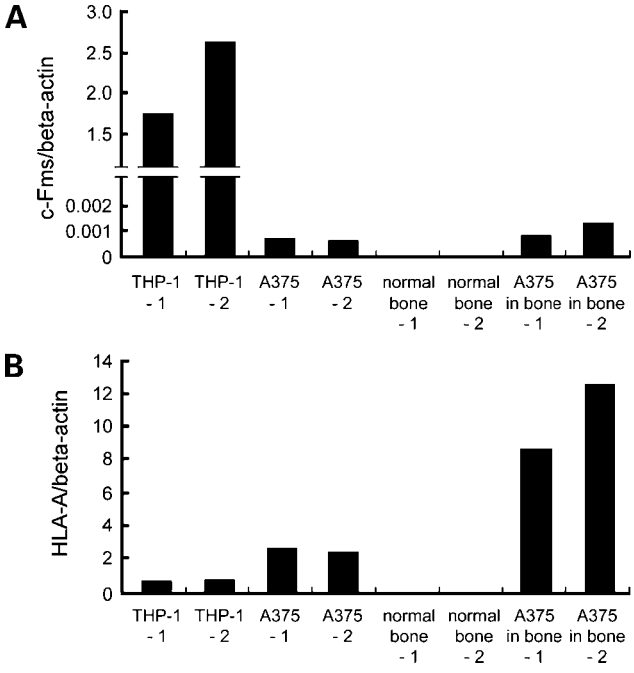

Figure 6. Analysis of c-fms expression in cultured cells and metastasized tumor. **A**, c-fms mRNA levels of bone with a metastasized tumor, normal bone, A375, and THP-1 cells were analyzed by real-time quantitative PCR. **B**, human HLA-A mRNA levels were also analyzed to guarantee the quality and quantity of total RNAs extracted from the A375-derived metastasized tumor in rat bone. The results were normalized by the corresponding internal human β-actin levels. The results were independently obtained from the left and right tibiae. *Columns,* average.

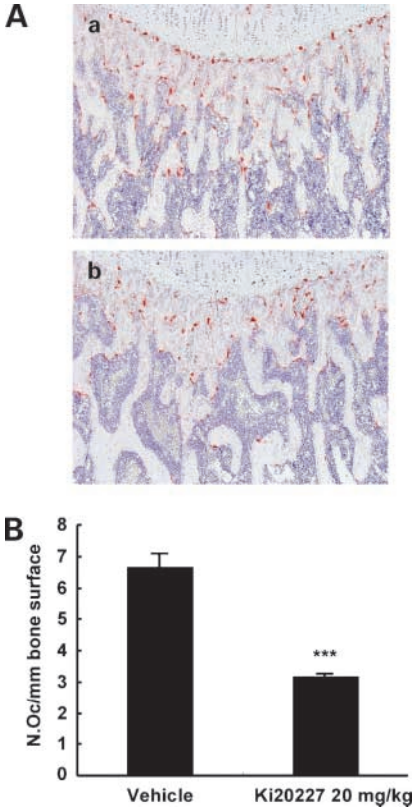

Figure 7. **A,** histologic appearance of TRAP-positive osteoclastic cells (*red*) in the primary spongiosa of vehicle-treated (**a**) and Ki20227-treated (20 mg/kg/d; **b**) ovx rats. The number of osteoclastic cells was found to be decreased in the Ki20227-treated bone. **B,** analysis of the number of osteoclastic cells (OcN/mm bone surface) in the primary spongiosa of both tibiae in either vehicle-treated or Ki20227-treated rats. Oral administration of Ki20227 was found to decrease the number of TRAP-positive osteoclastic cells. *Columns,* mean ($n = 6$ animals for each group); *bars,* SE. ***, $P < 0.001$, compared with vehicle-treated group.

If A375 cells in bone expressed c-Fms at higher levels than in culture, A375 cell growth in bone metastatic sites might be suppressed to a greater extent by Ki20227, as in the case of M-CSF-dependent M-NFS-60 cell growth. Phenotypic changes, such as growth factor production, have been observed in metastatic tumor cells in the bone microenvironment (30). Using quantitative PCR analysis, we found that human HLA-A expression levels between metastatic A375 cells in bone and in culture were different. The discrepancy in the HLA-A expression levels indicates the possibility of phenotypic changes in A375 within the bone microenvironment. However, c-Fms expression was not up-regulated in metastatic A375 in bone compared with A375 cells in culture. In addition, our cell-based assay data showed that Ki20227 did not suppress A375 growth *in vitro*. Therefore, we conclude that the inhibitory effects

of Ki20227 against osteolytic bone destruction and tumor colonization in bone are not mediated through a direct antiproliferative effect on metastatic A375. On the other hand, Ki20227 has inhibitory activity against KDR. It has also been reported that an angiogenesis inhibitor can suppress osteolytic bone metastasis (11). Therefore, KDR inhibition might contribute partially to the suppression of tumor colonization in bone.

To confirm the inhibitory activity of Ki20227 against the development of osteoclasts in no tumor-bearing animals, we examined a rat ovx model. Treatment with Ki20227 at a dose of 20 mg/kg/d for 28 days significantly decreased the number of TRAP-positive osteoclastic cells on the bone surface in the primary spongiosa. However, treatment with 20 mg/kg/d of Ki20227 did not significantly suppress osteolysis induced by A375 in a rat bone metastasis model. It may be that the administration of higher doses of Ki20227 decreases the number of osteoclastic cells in the ovx model to a greater extent. Kimble et al. reported that stromal cells from ovx mice produced larger amounts of M-CSF than stromal cells from estrogen-replete mice, and Cenci et al. found that anti-M-CSF-neutralizing antibody completely suppressed ovx-induced bone loss (34, 35). These data support the hypothesis that Ki20227 has the ability to suppress osteoclast development caused by ovariectomy *in vivo*. Thus, we believe that the inhibitory effects of Ki20227 during osteoclast development constitute substantial portion of its effects against the osteolytic bone resorption induced by metastatic A375 cells.

It has been indicated that M-CSF plays an important role, not only in osteoclast development and bone metastasis but also in tumor growth, tissue invasion, and malignancy (36–42). Marked elevations in serum M-CSF levels was found in patients with endometrial or ovarian cancer (36, 37). Additionally, it has been reported that M-CSF promotes tissue invasion by lung cancer cells by enhancing matrix metalloproteinase-2 production, that functional M-CSF deficiency delays mammary tumor progression and metastasis in *op/op* mice, and that overexpression of both M-CSF and c-Fms induces hyperplasia and tumor formation in the mammary glands (38–40). In therapeutic trials, M-CSF antisense oligonucleotide treatment suppressed the growth of colon and mammary cancers and small interfering RNAs inhibited mammary cancer growth in rodent xenograft models, supporting the idea that a blockade of M-CSF signaling is effective against various tumor growths and malignancies (41, 42).

In conclusion, we have shown that the c-Fms inhibitor Ki20227 decreases the number of osteoclasts both *in vitro* and *in vivo* and suppresses osteolysis induced by metastatic tumor cells. Thus, Ki20227 may be a potential anti-osteolytic agent in cases of metastatic disease or loss of gonadal function.

Acknowledgments

We thank Drs. K. Nakamura, T. Kobayashi, and T. Shimada for their excellent technical support and Drs. A. Miwa and T. Yamashita for their helpful suggestions.

References

1. Yoneda T. Cellular and molecular mechanisms of breast and prostate cancer metastasis to bone. Eur J Cancer 1998;34:240 – 5.

2. Guise TA, Yin JJ, Taylor SD, et al. Evidence for a causal role of parathyroid hormone-related protein in the pathogenesis of human breast cancer-mediated osteolysis. J Clin Invest 1996;98:1544 – 9.

3. Michigami T, Ihara-Watanabe M, Yamazaki M, Ozono K. Receptor activator of nuclear factor κB ligand (RANKL) is a key molecule of osteoclast formation for bone metastasis in a newly developed model of human neuroblastoma. Cancer Res 2001;61:1637 – 44.

4. Yin JJ, Selander K, Chirgwin JM, et al. TGF-β signaling blockade inhibits PTHrP secretion by breast cancer cells and bone metastases development. J Clin Invest 1999;103:197 – 206.

5. Sasaki A, Boyce BF, Story B, et al. Bisphosphonate risedronate reduces metastatic human breast cancer burden in bone in nude mice. Cancer Res 1995;55:3551 – 7.

6. Yoneda T, Sasaki A, Dunstan C, et al. Inhibition of osteolytic bone metastasis of breast cancer by combined treatment with the bisphosphonate ibandronate and tissue inhibitor of the matrix metalloproteinase-2. J Clin Invest 1997;99:2509 – 17.

7. Hiraga T, Williams PJ, Mundy GR, Yoneda T. The bisphosphonate ibandronate promotes apoptosis in MDA-MB-231 human breast cancer cells in bone metastases. Cancer Res 2001;61:4418 – 24.

8. Hiraga T, Tanaka S, Yamamoto M, Nakajima T, Ozawa H. Inhibitory effects of bisphosphonate (YM175) on bone resorption induced by a metastatic bone tumor. Bone 1996;18:1 – 7.

9. Honore P, Luger NM, Sabino MA, et al. Osteoprotegerin blocks bone cancer-induced skeletal destruction, skeletal pain and pain-related neurochemical reorganization of the spinal cord. Nat Med 2000;6:521 – 8.

10. Morony S, Capparelli C, Sarosi I, Lacey DL, Dunstan CR, Kostenuik PJ. Osteoprotegerin inhibits osteolysis and decreases skeletal tumor burden in syngeneic and nude mouse models of experimental bone metastasis. Cancer Res 2001;61:4432 – 6.

11. Sasaki A, Alcalde RE, Nishiyama A, et al. Angiogenesis inhibitor TNP-470 inhibits human breast cancer osteolytic bone metastasis in nude mice through the reduction of bone resorption. Cancer Res 1998;58:462 – 7.

12. Kodama H, Yamasaki A, Abe M, Niida S, Hakeda Y, Kawashima H. Transient recruitment of osteoclasts and expression of their function in osteopetrotic (op/op) mice by a single injection of macrophage colony-stimulating factor. J Bone Miner Res 1993;8:45 – 50.

13. Hughes DE, Wright KR, Uy HL, et al. Bisphosphonates promote apoptosis in murine osteoclasts *in vitro* and *in vivo*. J Bone Miner Res 1995;10:1478 – 87.

14. Simonet WS, Lacey DL, Dunstan C, et al. Osteoprotegerin: a novel secreted protein involved in the regulation of bone density. Cell 1997;89:309 – 19.

15. Yasuda H, Shima N, Nakagawa N, et al. Identity of osteoclastogenesis inhibitory factor (OCIF) and osteoprotegerin (OPG): a mechanism by which OPG/OCIF inhibits osteoclastogenesis *in vitro*. Endocrinology 1998;139:1329 – 37.

16. Lacey DL, Timms E, Tan HL, et al. Osteoprotegerin ligand is a cytokine that regulates osteoclast differentiation and activation. Cell 1998;93:165 – 76.

17. Yasuda H, Shima N, Nakagawa N, et al. Osteoclast differentiation factor is a ligand for osteoprotegerin/osteoclastogenesis-inhibitory factor and is identical to TRANCE/RANKL. Proc Natl Acad Sci U S A 1998;95:3597 – 602.

18. Nakagawa N, Kinosaki M, Yamaguchi K, et al. RANK is the essential signaling receptor for osteoclast differentiation factor in osteoclastogenesis. Biochem Biophys Res Commun 1998;253:395 – 400.

19. Anderson DM, Maraskovsky E, Billingsley WL, et al. A homologue of the TNF receptor and its ligand enhance T-cell growth and dendritic-cell function. Nature (Lond) 1997;390:175 – 9.

20. Yoshida H, Hayashi S, Kunisada T, et al. The murine mutation osteopetrosis is in the coding region of the macrophage colony stimulating factor gene. Nature (Lond) 1990;345:442 – 4.

21. Wiktor-Jedrzejczak W, Bartocci A, Ferrante AW, Jr., et al. Total absence of colony-stimulating factor 1 in the macrophage-deficient osteopetrotic (*op/op*) mouse. Proc Natl Acad Sci U S A 1990;87:4828 – 32.

22. Kodama H, Yamasaki A, Nose M, et al. Congenital osteoclast

deficiency in osteopetrotic (*op/op*) mice is cured by injections of macrophage colony-stimulating factor. J Exp Med 1991;173:269 – 72.

23. Felix R, Cecchini MG, Hofstetter W, Elford PR, Stutzer A, Fleisch H. Impairment of macrophage colony-stimulating factor production and lack of resident bone marrow macrophages in the osteopetrotic *op/op* mouse. J Bone Miner Res 1990;5:781 – 9.

24. Dai XM, Ryan GR, Hapel AJ, et al. Targeted disruption of the mouse colony-stimulating factor 1 receptor gene results in osteopetrosis, mononuclear phagocyte deficiency, increased primitive progenitor cell frequencies, and reproductive defects. Blood 2002;99:111 – 20.

25. Kobayashi K, Takahashi N, Jimi E, et al. Tumor necrosis factor α stimulates osteoclast differentiation by a mechanism independent of the ODF/RANKL-RANK interaction. J Exp Med 2000;191:275 – 85.

26. Laird AD, Cherrington JM. Small molecule tyrosine kinase inhibitors: clinical development of anticancer agents. Exp Opin Invest Drugs 2003; 12:51 – 64.

27. Sherr CJ. Regulation of mononuclear phagocyte proliferation by colony-stimulating factor-1. Int J Cell Cloning 1990;8 Suppl 1:46 – 60.

28. Fuller K, Owens JM, Jagger CJ, Wilson A, Moss R, Chambers TJ. Macrophage colony-stimulating factor stimulates survival and chemotactic behavior in isolated osteoclasts. J Exp Med 1993;178:1733 – 44.

29. Weir EC, Lowik CW, Paliwal I, Insogna KL. Colony stimulating factor-1 plays a role in osteoclast formation and function in bone resorption induced by parathyroid hormone and parathyroid hormone-related protein. J Bone Miner Res 1996;11:1474 – 81.

30. van der Pluijm G, Sijmons B, Vloedgraven H, Deckers M, Papapoulos S, Lowik C. Monitoring metastatic behavior of human tumor cells in mice with species-specific polymerase chain reaction: elevated expression of angiogenesis and bone resorption stimulators by breast cancer in bone metastases. J Bone Miner Res 2001;16:1077 – 91.

31. Nakai M, Mundy GR, Williams PJ, Boyce B, Yoneda T. A synthetic antagonist to laminin inhibits the formation of osteolytic metastases by human melanoma cells in nude mice. Cancer Res 1992;52:5395 – 9.

32. Hiraga T, Nakajima T, Ozawa H. Bone resorption induced by a metastatic human melanoma cell line. Bone 1995;16:349 – 56.

33. El Abdaimi K, Papavasiliou V, Goltzman D, Kremer R. Expression and regulation of parathyroid hormone-related peptide in normal and malignant melanocytes. Am J Physiol Cell Physiol 2000;279:C1230 – 8.

34. Kimble RB, Srivastava S, Ross FP, Matayoshi A, Pacifici R. Estrogen deficiency increases the ability of stromal cells to support murine osteoclastogenesis via an interleukin-1 and tumor necrosis factor-mediated stimulation of macrophage colony-stimulating factor production. J Biol Chem 1996;271:28890 – 7.

35. Cenci S, Weitzmann MN, Gentile MA, Aisa MC, Pacifici R. M-CSF neutralization and egr-1 deficiency prevent ovariectomy-induced bone loss. J Clin Invest 2000;105:1279 – 87.

36. Kacinski BM, Chambers SK, Stanley ER, et al. The cytokine CSF-1 (M-CSF) expressed by endometrial carcinomas *in vivo* and *in vitro*, may also be a circulating tumor marker of neoplastic disease activity in endometrial carcinoma patients. Int J Radiat Oncol Biol Phys 1990;19:619 – 26.

37. Kacinski BM, Stanley ER, Carter D, et al. Circulating levels of CSF-1 (M-CSF), a lymphohematopoietic cytokine, may be a useful marker of disease status in patients with malignant ovarian neoplasms. Int J Radiat Oncol Biol Phys 1989;17:159 – 64.

38. Pei XH, Nakanishi Y, Takayama K, Bai F, Hara N. Granulocyte, granulocyte-macrophage, and macrophage colony-stimulating factors can stimulate the invasive capacity of human lung cancer cells. Br J Cancer 1999;79:40 – 6.

39. Lin EY, Nguyen AV, Russell RG, Pollard JW. Colony-stimulating factor 1 promotes progression of mammary tumors to malignancy. J Exp Med 2001;19:727 – 40.

40. Kirma N, Luthra R, Jones J, et al. Overexpression of the colony-stimulating factor (CSF-1) and/or its receptor c-fms in mammary glands of transgenic mice results in hyperplasia and tumor formation. Cancer Res 2004;64:4162 – 70.

41. Aharinejad S, Abraham D, Paulus P, et al. Colony-stimulating factor-1 antisense treatment suppresses growth of human tumor xenografts in mice. Cancer Res 2002;62:5317 – 24.

42. Aharinejad S, Paulus P, Sioud M, et al. Colony-stimulating factor-1 blockade by antisense oligonucleotides and small interfering RNAs suppresses growth of human mammary tumor xenografts in mice. Cancer Res 2004;64:5378 – 84.